Q235B 钢对接焊接头振动 S－N 曲线的分析

范文学[1,2]， 陈芙蓉[1]， 解瑞军[1]， 唐大富[1]
(1. 内蒙古工业大学 材料科学与工程学院，呼和浩特 010051；2. 内蒙古工业大学 矿业学院，呼和浩特 010051)

摘 要：通过分析确定 Q235B 钢对接焊接头的振动疲劳 S－N 曲线与静疲劳 S－N 曲线是具有相同斜率的连续型曲线，并基于静疲劳 S－N 曲线推得振动疲劳 S－N 曲线的表达式. 文中通过试验确定了 Q235B 钢对接焊接头的静疲劳 S－N 曲线和不同加载频率下对应的真实拉伸强度，确定了振动疲劳修正系数为 0.345 2，经过残余应力和接头板厚修正后，利用振动疲劳 S－N 曲线预测了疲劳寿命为 5×10^6 周次时振动疲劳极限为 114.84 MPa，与试验值相差仅为 7.60%. 结果表明，文中所用方法能够用于 Q235B 钢振动 S－N 曲线的推断.

关键词：Q235B 钢；焊接接头；振动疲劳；S－N 曲线
中图分类号：TG 405 **文献标识码**：A **文章编号**：0253－360X(2014)08－0039－04

0 序 言

疲劳是焊接结构破坏的主要形式之一，基于应力—寿命(S－N)曲线进行疲劳寿命预测的方法，可统称为 S－N 曲线法，它是疲劳评定中常用的方法. 常规疲劳，即静疲劳试验一般均在较低频率下完成，且得到疲劳寿命 S－N 曲线在 $2\times10^6\sim5\times10^6$ 周次后出现一水平段，即所谓的条件疲劳极限. 然而当外加载荷频率达到试样共振频率时，S－N 曲线的水平段消失，取而代之的是“连续下降”[1,2] 或“二次下降”[3,4] 的形式. 针对不同激励频率下的 S－N 曲线特性，薛红前等人[5] 研究了外加载荷频率为 30 Hz 的静疲劳和 20 kHz 的共振疲劳下 S－N 曲线的特点，发现在 $1\times10^5\sim1\times10^7$ 周次之间 100C6 高强度钢在两种频率下的疲劳试验数据很接近，而 D38MSV5S 钢振动 S－N 曲线在应力轴方向有较大的下移. 尹丹青等人[6] 对 Q235 钢和 16Mn 钢焊接接头在振动频率下的 S－N 曲线进行分析，结果表明两种材料焊接接头在 2×10^6 周次之后并未出现水平段，都为一条连续下降的曲线. 王弘、闫桂玲等人[3,4] 对 50 车轴钢和 40Cr 钢在静频率和共振频率下的 S－N 曲线进行研究，提出了频率影响因子，实现了不同频率间 S－N 曲线的相互转化. 对于 Q235B 钢焊接接头在不同频率下 S－N 曲线间的相互关系，目前讨论较少，为此文中对 Q235B 钢对接焊接头在不同频率下的 S－N 曲线进行分析，通过静疲劳 S－N 曲线推导出振动疲劳 S－N 曲线，并完成焊接接头疲劳寿命的预测，同时验证振动疲劳 S－N 曲线的准确性及可行性.

收稿日期：2013－10－18
基金项目：教育部春晖计划资助项目(Z2006-1-01003)

1 静疲劳与振动疲劳 S－N 曲线的分析

Q235B 钢对接焊接头的静疲劳指在远低于共振频率下进行的疲劳测试，其测试频率一般小于 150 Hz. 这类疲劳由于测试频率较低，一般的疲劳设备都具备相应的功能，常用于高周疲劳问题，所得 S－N 曲线可用幂函数方程表达，即

$$\Delta\sigma^m N = C \tag{1}$$

式中：$\Delta\sigma$ 为应力范围；N 为该应力下的疲劳寿命；m，C 为材料参数.

式(1)的对数形式可以表达为

$$m\lg\Delta\sigma = \lg C - \lg N \tag{2}$$

振动疲劳是在共振状态下完成测试，所以测试频率较高. 根据文献[1－5]中试验数据拟合所得振动疲劳 S－N 曲线，其倾斜方向与静疲劳 S－N 曲线近似相同，即 S－N 曲线的斜率近似相同，只是相同疲劳寿命下所对应的应力发生了一定的变化，即在双对数坐标系中 S－N 曲线在应力轴方向上进行移动，相当于式(2)右侧部分加了一个系数. 由文献[7]可知，S－N 曲线公式中的参数 m 和 C 均为随机变量，但由于斜率 m 的稳定性较强一般分析中将 m 视为确定值，而将 C 作为变量进行处理. 所以假设振动疲劳 S－N 曲线的表达式为

$$m\lg\Delta\sigma = C_1 + C_2 - \lg N \tag{3}$$

式中：C_1 为 $\lg C$；设 C_2 为振动疲劳修正系数.

2 振动疲劳 S－N 曲线参数的确定

根据式(3)可知,确定 C_2 便可推断获取振动疲劳 S－N 曲线. 通过对文献[3]的分析可知,同种材料在不同加载频率下,相同循环周次对应的条件疲劳极限比值与 S－N 曲线的 Basquin 表达式中的疲劳强度系数近似相等,即频率影响系数(F_E)为

$$F_E = \frac{\sigma_s}{\sigma_v} \approx \frac{\sigma'_{fs}}{\sigma'_{fv}} \tag{4}$$

式中:σ_s 为静条件疲劳极限;σ_v 为振动条件疲劳极限;σ'_{fs}为静疲劳强度系数;σ'_{fv}为振动疲劳强度系数.

而疲劳强度系数与多数金属材料经过颈缩修正后的真实断裂强度 σ_f 接近[8],即

$$F_E = \frac{\sigma'_{fs}}{\sigma'_{fv}} = \frac{\sigma_{fs}}{\sigma_{fv}} \tag{5}$$

式中:σ_{fs}为静疲劳试验频率对应的断裂强度;σ_{fv}为振动疲劳试验频率对应的断裂强度. 由此复杂的疲劳试验问题就可以通过简单的拉伸试验解决.

结合式(2),式(3),式(5)可得振动疲劳修正系数,即

$$C_2 = m\lg(\sigma_v - \sigma_s) = m\lg\frac{1}{F_E} \tag{6}$$

3 Q235B 钢静疲劳 S－N 曲线的确定

3.1 试验材料及试验制备

拉伸试验采用 8 mm 厚的 Q235B 钢板,焊条采用 E5015,直径均为 4 mm,其力学性能见表 1.

表 1 试验材料的力学性能

Table 1 Mechanical properties of test materials

材料	屈服强度 R_{eL}/MPa	抗拉强度 R_m/MPa	弹性模量 E/GPa	泊松比 λ
Q235B	265	415	206	0.26
E5015	457	552	210	0.30

采用直流反接电弧焊实施双面双层焊接,焊接时从坡口一端起弧到另一端熄弧,避免中部起、熄弧. 层间温度 110 ℃,防止焊接咬边的产生,坡口边缘应填满液态金属. 焊接工艺参数见表 2. 图 1 为接头试样尺寸.

表 2 对接焊工艺参数

Table 2 Welding parameters of butt welded joints

	焊条直径 d/mm	焊接电流 I/A	电弧电压 U/V	焊接速度 v/(mm·min^{-1})
第一层	4.0	135	22～24	200
第二层	4.0	155	23～25	150

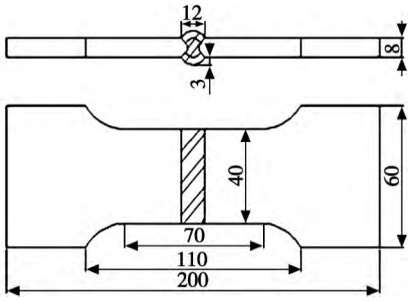

图 1 对接接头的几何形状和尺寸(mm)

Fig. 1 Geometical characteristic of butt joints

3.2 疲劳试验及数据处理

表 3 为疲劳试验数据. 疲劳试验是在 GPS300 型高频疲劳试验机上进行. 应力循环比为 0.1,振动频率控制在 130～140 Hz 的范围内.

表 3 疲劳试验数据

Table 3 Data of fatigue test

样件编号	应力范围 $\Delta\sigma$/MPa	疲劳寿命 N(10^6 周次)	断裂位置
1	160	2.752	焊趾
2	170	1.886	焊趾
3	175	1.645	焊趾
4	180	1.415	焊趾
5	190	1.780	焊趾
6	210	0.778	焊趾
7	230	0.328	焊趾

试验疲劳数据采用最小二乘法回归计算进行处理后[9],得到存活率为 50% 的中值 S－N 曲线的表达式,即

$$\lg N = 18.23 - 5.34\lg\Delta\sigma \tag{7}$$

由图 2 知,疲劳寿命为 5×10^6 周次时,对应的静疲劳极限为 171.35 MPa.

4 Q235B 钢振动疲劳 S－N 曲线的确定

为了选择合适的应变速率,首先通过有限元技术对静疲劳的试件进行模态分析,确定试件发生共振时的频率为 1.79 kHz.

试验在 INSTRON 公司的高应变速率 VHS160/100－20 试验机上进行. 依据国家标准 GB/T228.1－2010《金属材料拉伸试验第 1 部分: 室温试验方法》[10] 控制不同频率、不同应力范围下所对应的应变速率($\dot{\varepsilon}_{max}$)[3],即

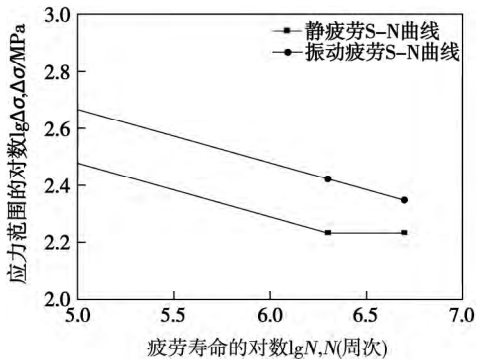

图 2　对接接头的 S－N 曲线

Fig. 2　S－N curve of butt joints

$$\dot{\varepsilon}_{max} = \pi f \frac{\Delta\sigma}{E} \tag{8}$$

式中: f 为加载频率; E 为弹性模量. 拉伸结果如表 4 所示.

表 4　拉伸试验数据

Table 4　Data of tensile test

加载频率 f/Hz	应力范围 $\Delta\sigma$/MPa	应变速率 $\dot{\varepsilon}_{max}$/s^{-1}	断裂强度 σ_f/MPa		频率影响系数 F_E
135～145	230	0.508	342.68	342.937	0.861 7
	190	0.420	338.83		
	160	0.354	347.30		
17 000～18 000	370	98.697	395.02	397.970	0.861 7
	240	64.019	397.87		
	210	56.017	401.02		

对照表 4 数据，可见随着加载频率的增加，材料的断裂强度有所增加，这与文献所述一致. 由式(5)可得频率影响系数为 0.861 7，带入式(6)可得 C_2 = 0.345 2. 结合 C_2 值及 Q235B 钢静疲劳 S－N 曲线式(7)可得 Q235B 钢振动 S－N 曲线表达式为

$$\lg N = 18.58 - 5.34\lg\Delta\sigma \tag{9}$$

疲劳寿命为 5×10^6 周次时，对应的振动疲劳极限为 167.85 MPa. 振动疲劳 S－N 曲线如图 2 所示.

5　振动疲劳 S－N 曲线的验证

根据以上推断，当 Q235B 钢对接焊接头承受疲劳寿命为 5×10^6 周次时，对应的振动疲劳极限为 167.85 MPa. 这个值是否正确，需要对其进行验证，由于文中对应焊接接头未完成振动疲劳试验，所以以文献[10]中提供数据进行验证. 而文献[10]给定疲劳寿命为 5×10^6 周次时的振动疲劳极限为 219.18 MPa，两者相差太大，说明简单的频率修正后的振动疲劳 S－N 曲线还不能完全应用于实际工程，需对其进行必要的修正.

由于文中焊接接头尺寸、接头形式与文献[10]不同，且试验所采用的应力比不同，这是产生较大误差的根本原因.

疲劳分析中不同尺寸焊接接头中存在的残余应力不同，所以应该按照国际焊接学会的标准进行疲劳强度的修正，以达到修正振动疲劳 S－N 曲线的目的. 其修正方式按照疲劳强度的应力比修正，即

$$f(R) = \begin{cases} 1.6, & R < -1 \\ -0.4R + 1.2, & -1 \leqslant R \leqslant 0.5 \\ 1, & R > 0.5 \end{cases} \tag{10}$$

式中: $f(R)$ 为疲劳强度残余应力修正系数; R 为应力比.

文中残余应力修正系数 $f(R_1)$ = 1.16，文献[10]中残余应力修正系数 $f(R_2)$ = 1.6. 同时针对焊接接头板厚形式，按照国际焊接学会给定板厚式(11)进行修正，即

$$f(t) = \left(\frac{25}{t_{\text{eff}}}\right)^a \tag{11}$$

式中: $f(t)$ 为疲劳强度尺寸修正系数; t_{eff} 为有效板厚. 文中板厚修正系数 $f(t_1)$ = 1.26，文献[10]中板厚修正系数 $f(t_2)$ = 1.41; a 为板厚修正指数.

修正后疲劳寿命为 5×10^6 周次时，对应的振动疲劳极限如表 5 修正前后疲劳强度的比较.

表 5　修正前后疲劳强度的比较

Table 5　Data of tensile test

	疲劳强度 σ_v/MPa	修正后疲劳强度 σ_{vb}/MPa	误差
文中接头	167.85	114.84	7.60%
文献[10]接头	280.43	124.30	

由表 5 可见，经过修正后的振动疲劳强度与文献[10]中试验的疲劳强度偏差较小，对接焊接头的误差只有 7.60%，通过与试验数据对比说明文中提到的 Q235B 钢对接焊接头静疲劳 S－N 曲线推导振动疲劳 S－N 曲线的方法是可行的，能够用于 Q235B 钢对接焊接头振动疲劳寿命的预测.

6　结　　论

(1) 通过分析得到了 Q235B 钢对接焊接头静疲劳 S－N 曲线与振动疲劳 S－N 曲线间的频率关系.

(2) 通过对应频率下的材料拉伸强度确定了疲劳修正系数 C_2，并得到 C_2 = 0.345 2.

(3) 通过与试验数据比较,经修正后的振动疲劳 S－N 曲线具有较高的准确性.

参考文献:

[1] 吴良晨,王东坡,邓彩艳,等. 超长寿命区间 16Mn 钢焊接接头疲劳性能 [J]. 焊接学报,2008,29(3):117－120.
Wu Liangchen, Wang Dongpo, Deng Caiyan, *et al*. Fatigue properties of welded joints of 16Mn steel in super long life region [J]. Transactions of the China Welding Institution, 2008, 29(3): 117－120.

[2] 方冬慧,刘永杰,陈宜言,等. Q345 桥梁钢焊接接头超高周疲劳性能 [J]. 焊接学报,2011,32(8):77－80.
Fang Donghui, Liu Yongjie, Chen Yiyan, *et al*. Ultra-high cycle fatigue behavior of Q345 bridge steel welded joint [J]. Transactions of the China Welding Institution, 2011, 32(8): 77－80.

[3] 王 弘,高 庆. 超声疲劳试验中载荷频率对材料疲劳性能的影响 [J]. 理化检验－物理分册,2005,41(9):433－435.
Wang Hong, Gao Qing. Effect of load frequency on fatigue behabior of material in ultrasonic fatigue testing [J]. PYCA(Part: a physicstest test), 2005, 41(9): 433－435.

[4] 闫桂玲,王 弘,高 庆. 超声频率加载下 50 车轴钢超长寿命疲劳性能研究 [J]. 中国铁道科学,2004,25(2):78－81.
Yan Guiling, Wang Hong, Gao Qing. On ultra-long life fatigue behavior of 50 axle steel under ultrasonic frequency [J]. China Railway Science, 2004, 25(2): 78－81.

[5] 薛红前,陶 华. 20 kHz 频率下高强度钢超高周疲劳研究 [J]. 机械工程材料,2005,29(5):12－15.
Xue Hongqian, Tao Hua. Super high cycle fatigue of high strength steels at a frenquency of 20 kHz [J]. Materials for Mechanical Engineering, 2005, 29(5): 12－15.

[6] 尹丹青,王东坡,刘 哲. Q235 钢和 16Mn 钢接头超长寿命疲劳行为及疲劳寿命设计 [J]. 天津大学学报,2009,42(6):513－517.
Yin Danqing, Wang Dongpo, Liu Zhe. Ultra-long life fatigue behavior and fatigue life design of joint between steel Q235 and steel 16Mn [J]. Journal of Tianjin Unversity, 2009, 42(6): 513－517.

[7] 彭修宁,韦斌凝,薛建阳. 产生坑蚀后建筑用钢筋 S－N 曲线中 C 参数劣化规律的研究 [J]. 西安建筑科技大学学报,2009,41(5):627－630.
Peng Xiunin, Wei Binning, Xue Jianyang. Study on the deterioration of parameter C in S－N curve of steel bars with corrosion-pits used in construction [J]. Journal of Xi'an University of Architecture & Technology, 2009, 41(5): 627－630.

[8] Suresh S. 材料的疲劳 [M]. 王中光,译. 北京:国防工业出版社,1993.

[9] Hobbacher A. Recommendations for fatigue design of welded joints and components [M]. German: International Institute of Welding, 2002.

[10] 吴良晨. 超声频分量双周疲劳载荷作用下焊接接头的疲劳性能 [D]. 天津:天津大学,2008.

作者简介: 范文学,男,1981 年出生,博士研究生,讲师. 主要从事焊接疲劳和数控加工方面的科研和教学工作. 发表论文 5 篇. Email: fwx201878@163.com

通讯作者: 陈芙蓉,女,教授. Email: cfr7075@163.com

[上接第 34 页]

[8] Ruo Zhang, Ping Sing Tsai, James Edwin Cryer, *et al*. Shape from shading: a survey [J]. IEEE Transactions on Pattern Analysis and Machine Intelligence, 1999, 21(8): 119－131.

[9] Habert S. A novel method for an automatic 3D reconstruction of coronary arteries from angiographic images [C] // 2012 11th International Conference on Information Science, Signal Processing and their Applications (ISSPA), Montreéal, QC, Canada, 2012: 484－489.

[10] Oren M, Nayar S K. Generalization of Lambert's reflectance model [C] // Proceedings of the 21st Annual Conference on Computer Graphics and Interactive Techniques, New York, 1994: 239－246.

[11] Cook R L, Torrance K E. A reflectance model for computergraphics [J]. Computer Graphics, 1981, 15(3): 307－316.

[12] 赵辉煌,周德俭,吴兆华,等. 基于小波包变换与自适应阈值的 SMT 焊点图像 [J]. 焊接学报,2011,32(11):73－76.
Zhao Huihuang, Zhou Dejian, Wu Zhaohua, *et al*. SMT solder joint image denoising based on wavelet packet transform and adaptive threshold [J]. Transactions of the China Welding Institution, 2011, 32(11): 73－76.

作者简介: 赵辉煌,男,1982 年出生,博士,副教授. 主要从事计算机视觉、三维重建、图像处理、微电子组装检测等方面研究. 发表论文 30 余篇. Email: betterlife008@163.com

method data, the turning point of S－N curve requires turning transition. In order to make the S－N curve and the breaking point N_0 have more engineering application value, the theory and method of transition point connected with variable slope curve was proposed. The feasibility of using variable slope method has been verified by experiment, and the two curves were compared by analysis . The results show that the new method of drawing the S－N curve can display the performance of welding joints spot more accurately.

Key words: spot welded joints; S－N curve; breaking point N_0; variable slope slash transition

Analysis of vibration fatigue S－N curve on Q235B steel butt welded joint FAN Wenxue[1,2], CHEN Furong[1], XIE Ruijun[1], TANG Dafu[1] (1. Institute of Materials Science and Engineering, Inner Mongolia University of Technology, Hohhot 010051, China; 2. Mining Institute, Inner Mongolia University of Technology, Hohhot 010051, China). pp 39－42

Abstract: The interrelation of static fatigue S－N curve and vibration fatigue S－N curve on Q235B steel butt welded joints has been analyzed. The result shows they have the same slope, and vibration fatigue S－N curve is a continuous curve without horizontal section. It moves a specified distance in stress axis. At the same time, the vibration fatigue S－N curve expression was input. In this paper, the static fatigue test and tensile test under different load frequency were done. And vibration fatigue correction factor was 0.345 2. Through correction of residual stress and size, the fatigue limit was 114.84 MPa when the cycles were 5×10^6 under vibration fatigue S－N curve. And it only has a little bias 7.60%, it shows that the method of this paper can be used to infer vibration fatigue S－N curve of Q235B steel.

Key words: Q235B steel welded joint; vibration fatigue; S－N curve

Formation process of hot cracking in copper He shielding gas tungsten welding LI Yinan[1], YAN Jiuchun[2], GUO Feng[1], PENG Zilong[1] (1. Department of Mechanical Engineering, Qingdao Technological University, Qingdao 266033, China; 2. State Key Laboratory of Advanced Welding Production Technology, Harbin Institute of Technology, Harbin 150001, China). pp 43－47

Abstract: The formation mechanism of hot cracking in gas tungsten arc welding (GTAW) of copper structures in large dimensions was researched. The dynamic formation process of hot cracking was observed and analyzed. The formation criterion of hot cracking was optimized based on the Prokhorov's theory, and the finite element model of thick copper plates in GTA welding was established based on the rigid restraint cracking test. It is concluded that the internal deformation rate $\Delta\varepsilon$ is the internal reason of forming hot cracking. The variation of the transverse tensile stress and the $\Delta\varepsilon$ in brittle temperature range (BTR) was obtained. And the formation mechanism of hot cracking without preheating was carried out compared $\Delta\varepsilon$ with high temperature ductility of HS201 welded metal. The variation of $\Delta\varepsilon$ in difference preheating temperature was analyzed to prevent hot cracking forming, and it can be concluded that the $\Delta\varepsilon$ in BTR could be declined by preheating process and the cracking susceptibility will be decreased.

Key words: copper; hot cracking; gas tungsten arc welding

Modeling and control of the nonlinear joints system of mobile repair welding robot LIU Jiajun[1], SUN Zhenguo[1], ZHANG Wenzeng[1], CHEN Qiang[1,2] (1. Key Laboratory for Advanced Materials Processing Technology, Department of Mechanical Engineering, Tsinghua University, Ministry of Education, Beijing 100084, China; 2. Yangtze Delta Region Institute of Tsinghua University, Jiaxing 314006, China). pp 48－52

Abstract: Highly nonlinear units such as deadzone and backlash exist in the joints of mobile repair welding robot, which have negative effects on control accuracy. To improve the path control accuracy of the end effector, Particle swarm optimization algorithm is used to identify the model of the nonlinear joints system. Then switching compensation control method referring the identified model is applied to the joint controlling system, combined with feedfoward-feedback control based on inverse kinematics, the hybrid control method realize considerable path accuracy. Experiments show that the average path error of designed welding robot's end effector is less than 0.2 mm with this control method, and the shortcomings of low precision reducer are compensated.

Key words: mobile welding robot; nonlinear system; identification; backlash compensation; feedforward

Feature characters extraction with visual attention method based on three-light-path weld pool images ZHANG Yan, LÜ Na, HUANG Yiming, CHEN Shanben (Intelligentized Robotic Welding Technology Laboratory, Shanghai Jiaotong University, Shanghai 200240, China). pp 53－56

Abstract: Seam tracking and weld penetration control are key parts of weld quality control. A three-light-path vision sensing system is used in the experiments to obtain the images of the top-front, top-back and back paths of the weld pool during the Al alloy GTAW welding and project them in the same picture at the same time. The image contains information of the seam, weld pool and back weld pool. The method of visual attention is adopted to find the small areas related to weld pool feature characters, and extract these characters from the image. The results show that, in real-time detection of the weld pool features during the welding process, the method of visual attention is more clarified and efficient than general methods as it focuses only on interested small areas.

Key words: welding quality control; weld pool image processing; visual attention; region of interest detection

Investigation on three-dimensional real coupling numerical simulation of temperature field of friction stir welding of 2219 aluminum alloy DU Yanfeng[1,2], BAI Jingbin[1], TIAN Zhijie[1], LI Jinsong[1], ZHANG Yanhua[2] (1. Capital Aerospace